AGU PUBLICATIONS

Radio Science

RESEARCH ARTICLE
10.1002/2014RS005476

Special Section:
URSI Symposium on Radiowave Propagation and Remote Sensing, 2013

Key Points:
- Spatial rain rate data have been analyzed to derive correlation coefficients
- The study is of particular importance for satellite site diversity
- A new site diversity prediction model has been developed

Correspondence to:
T. Tjelta,
terje.tjelta@telenor.com

Citation:
Tjelta, T., J. Mamen, L. E. Bråten, and P. A. Grotthing (2014), Measured and modeled spatial rain rate correlation to improve the prediction method for satellite site diversity, *Radio Sci.*, *49*, 1232–1244, doi:10.1002/2014RS005476.

Received 27 APR 2014
Accepted 18 NOV 2014
Accepted article online 25 NOV 2014
Published online 17 DEC 2014

Measured and modeled spatial rain rate correlation to improve the prediction method for satellite site diversity

Terje Tjelta[1,2], Jostein Mamen[3], Lars Erling Bråten[2,4], and Per Arne Grotthing[5]

[1]Telenor, Fornebu, Norway, [2]University Graduate Center, Kjeller, Norway, [3]Norwegian Meteorological Institute, Oslo, Norway, [4]Norwegian Defence Research Establishment (FFI), Kjeller, Norway, [5]Telenor Satellite Broadcasting, Fornebu, Norway

Abstract Rainfall rate varies both temporarily and spatially. Radio systems, where rain attenuation causes outages, may take advantage of this effect to increase the radio link or satellite link availability using diversity techniques. In the Oslo region with Norwegian Meteorological Institute located at Blindern, there are 24 tipping bucket rain gauges within 50 km radius of the institute where each station has 5 years or more of simultaneous data periods with the station at the institute. The simultaneous data have been used to calculate spatial rain rate correlation and derive a prediction method based on separation distance and orientation with respect to dominating weather direction. Part of joint rain rate distribution was fitted to lognormal to find the measured correlation coefficients. In addition, an analysis of independent radiosonde data suggests that prevailing wind at 700 hPa or 850 hPa altitude (approximately 3000 m or 1500 m above sea level), conditioned thunderstorm index in the range of 15 to 20, may be used to identify the actual rainfall movement or dominant weather direction. Compared with current recommended method by the Radiocommunication Sector of International Telecommunication Union, the new method gives an improved site diversity prediction judged by site selection of minimum 20 GHz attenuation data measured in 2012 from Earth stations located at Nittedal and Kjeller separated by 23 km.

1. Introduction

Rainfall varies both temporarily and spatially, and radio systems affected by rain attenuation may take advantage of this effect to reduce the rain caused by degraded performance and availability. This applies to both terrestrial and Earth-space links. Link availability improvement prediction methods using path diversity for terrestrial links and site diversity for satellite links have been developed taking advantage of noncorrelated attenuation. These methods used indicate that simultaneous rainfall intensity is different at the radio system's terminal locations. The Radiocommunication Sector of International Telecommunication Union (ITU-R) recommend prediction methods in P.618 [*Radiocommunication Sector of International Telecommunication Union* (*ITU-R*), 2013a], P.1410 [*ITU-R*, 2012], and P.530 [*ITU-R*, 2013b] are based on modeling the rain attenuation and rainfall rate to follow lognormal distributions. The ITU-R-recommended procedure for satellite site diversity in P.618 [*ITU-R*, 2013a] uses the distance between the sites, a correlation coefficient of rain rate at the two different sites, and a correlation coefficient for rain attenuation at the two different sites to predict the site diversity improvement. For radio communication systems, the interest is in finding the percentage of time the attenuation exceeds system thresholds for all the diversity paths and for satellite communication finding, the time the attenuation exceeds the thresholds at the two sites simultaneously.

This article deals with the correlation of rainfall at two sites, which is part of the P.618 procedure for satellite site diversity. It does this by analyzing tipping bucket rain gauge data from the Oslo region and deriving a model for the rain rate correlation coefficient. The current model of rain correlation coefficient in P.618 depends only on site separation distance. In looking for further improvement of site diversity prediction methods, the site's baseline angle with a dominant weather direction has been included in the work presented in this article. The weather direction has been found by analyzing the dense rain gauge network data. However, searching for an independent way of determining the dominant weather direction, additional radiosonde data from a station in the Oslo region have been studied. It seems possible that

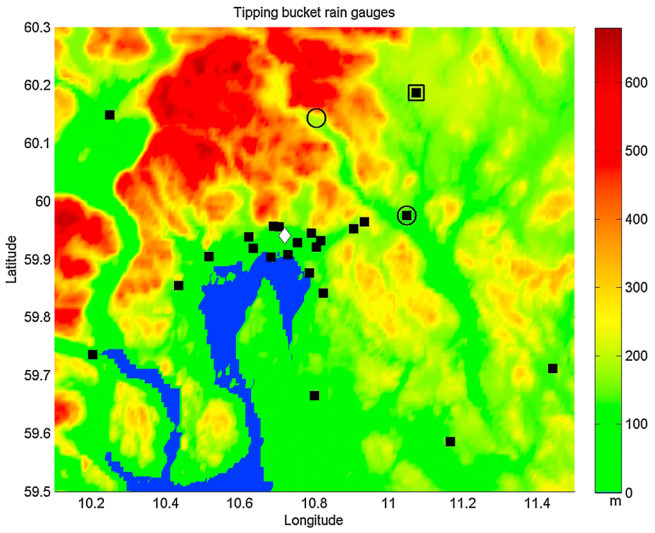

Figure 1. Tipping bucket rain gauge locations where Blindern is marked white diamond, the other gauges as black squares, the two Earth stations Nittedal (most North) and Kjeller locations as circles, and radiosonde location at Gardermoen by a nonfilled square co-located with one of the rain gauges.

radiosonde data that can support the model of correlation depended on separation distance and angle with respect to a prevailing weather direction. One example of the diversity improvement is calculated and compared with measurements from two different sites for 20 GHz satellite links shows very good correspondence.

The article is organized in six main sections with the introduction in section 1, description of the measurement rain gauge stations and measured data analyses in section 2, development of the prediction methods for rain correlation coefficient in section 3, analysis of local meteorological and climate with radiosonde data in section 4 in search for support of findings in section 3, comparison with measured 20 GHz satellite site diversity rain attenuation data in section 5, and discussion and conclusion in section 6.

2. Measured Spatial and Temporal Rain Intensity

In the Oslo region with Norwegian Meteorological Institute located at Blindern, there is a quite dense network of tipping bucket rain gauges where long-term data records are available from the institute's databases. The tipping bucket rain gauges used in the investigation are located as shown in Figure 1 with longitudes and latitudes indicated. The terrain elevation given in the bar code at the right shows altitudes from sea level to above 600 m with the sea level colored in blue showing the Oslofjord. Since the latitude is around 60° and the longitude spans double in degrees as the latitude, the distances between stations measured from the square-formatted figure are directly comparable. The rain gauge stations used in the study are spread over the whole area and marked with filled black squares except the one at Blindern shown as a filled white diamond. The highest station density is within the city of Oslo somewhat more concentrated along the west-east direction. The open larger square is the location of the radiosonde station at Gardermoen, co-located with one of the rain gauges (section 4). The two open circles are the satellite Earth stations at Nittedal and Kjeller with measurement performed at 20 GHz (section 5) where Kjeller is co-located with one of the rain gauge stations.

The rain gauge stations marked as black squares are the selected ones within 50 km distance from Blindern that is marked as a white diamond. For each pair of stations, there exists a period of time when both stations have been operated. The data for each pair have been selected to ensure that the distribution of minimum rain rate from each pair gives result that covers or is close to the 0.01% of the period. Furthermore, to ensure enough simultaneous and satisfactory quality data, the following criteria were used when choosing station data sets from stations within 50 km from Blindern:

1. Minimum 5 years common data period.
2. The data in selected years must include the dominating rainy period of summer and early fall.
3. Each year data were accepted if the number of observations for one station was within 0.5 to 2 times the number of observations for the other station.
4. The rain gauge bucket size must be the same for both stations, i.e., either only 0.1 mm bucket or 0.2 mm bucket for a pair. Note that most stations have been upgraded from 0.2 mm bucket size to 0.1 mm bucket size.

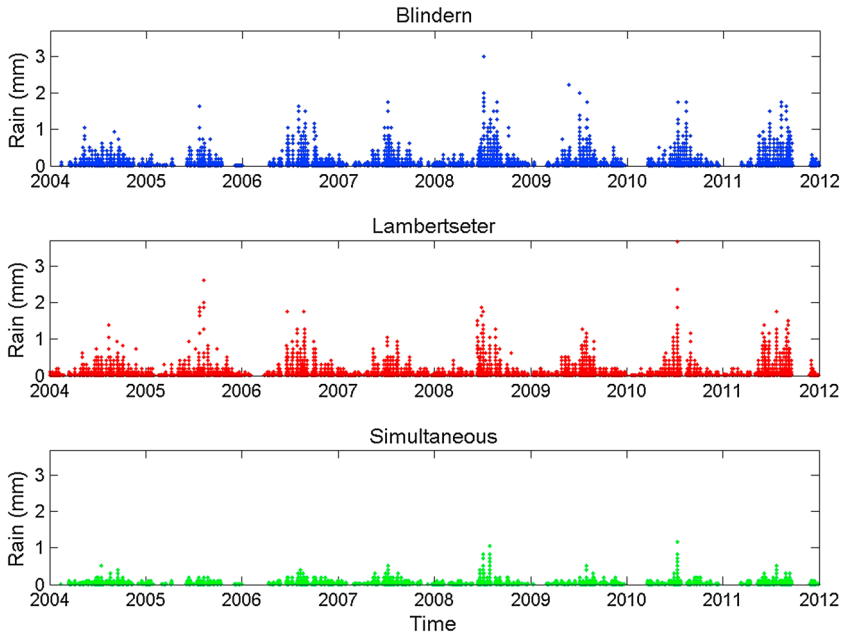

Figure 2. Clock minute rainfall observations at Blindern and Lambertseter in Oslo along with at the any instant simultaneous minimum value.

Figure 2 illustrates an example of clock minute observations of rainfall from the period of 2004 to 2011 for Blindern and Lambertseter and minimum of simultaneous observations. The data are available as measured rainfall in millimeter per clock minute. It is easily seen that the minimum of two provides a time series with significant lower measured rain, but this plot does not allow inspection of nonrainy periods due to the small space and large dots.

Table 1. Some Characteristics of Rain Gauge Simultaneous Data Sets Used in the Study

		Number of Minute Data Per Year From Station 18701 (Blindern) Divided by the Number of Minute Data Per Year From the Stations Listed			
Station	No. of Years	Mean	Minimum	Maximum	Standard Deviation
2840	12	1.2	0.9	1.7	0.23
3810	23	1.2	0.9	1.8	0.28
4220	11	1.2	0.9	1.8	0.25
4781	28	1.2	0.9	1.8	0.25
17870	22	1.1	0.6	1.7	0.31
17980	7	1.0	0.6	1.7	0.30
18020	8	1.0	0.6	1.7	0.30
18190	6	1.1	0.6	1.7	0.31
18210	8	1.1	0.6	1.7	0.29
18269	8	1.0	0.6	1.7	0.31
18270	18	1.0	0.6	1.6	0.30
18320	7	1.1	0.6	1.6	0.30
18420	8	1.0	0.6	1.6	0.30
18640	12	1.1	0.6	1.6	0.29
18815	7	1.1	0.6	1.7	0.31
18920	7	1.0	0.6	1.6	0.30
18980	7	1.0	0.6	1.6	0.29
19490	18	1.0	0.6	1.6	0.24
19510	21	1.1	0.6	1.6	0.24
19710	17	1.0	0.6	1.6	0.25
20300	12	1.2	0.6	1.9	0.36
24130	5	1.2	0.6	1.9	0.32
26890	23	1.1	0.7	1.8	0.27

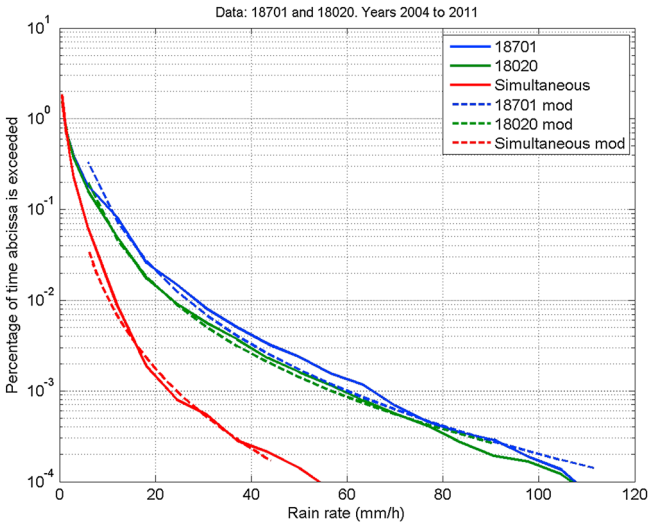

Figure 3. Individual station and the minimum rain rate distributions for common data from Blindern and Lambertseter showing the percentage of the average year the rain rate is exceeded on each of the sites and for both sites.

Table 1 provides some characteristics of the data selected by the criteria above. Each of the stations in the list forms a pair with Station 18701 (Blindern). For each year of concurrent data, there are a number of clock minutes with observed precipitation. Characteristics of the ratio of the number from Station 18701 divided by the numbers of clock minute date from each of the other stations are tabulated. It is seen that on average, the number of clock minutes are equal or close, but some variability exists. The main cause of variability is that some series of winter precipitation from one station were not available for the other. The winter precipitation has a shallow intensity in this region [*Tjelta and Mamen*, 2014] and has a limited impact on the results in this article.

For each individual station and for the instantly minimum rain observed by the pair, the time series data have been used to find rain rate distributions for the full common period using the recently published algorithm by *Mamen and Tjelta* [2013]. Tipping bucket data from the meteorological institute are measured as the number of tips per clock minute and then converted to millimeter water according to the actual instrument used, such as bucket size and dead time accounting for the time it takes to get an empty bucket in position for a new measurement. The algorithm used for analyzing the clock minute tipping bucket rain rate distributions converts data back to the number of tips per clock minute. The one-tip cases are handled by taking the time to the previous observation (or start time) into consideration; i.e., as an example, if there was 8 min with no counts before a one-tip observation, the one-tip is split onto 8 times of 1/8 of the bucket size (0.1 mm or 0.2 mm). This procedure enables an analysis to estimate the shallow rainfall rate distribution. The simple method assumes that the shallow rainfall intensity is constant in the period it takes to fill the first bucket. Still, the distribution is discrete but with expanded one-tip cases onto 1, 1/2, 1/3, and so on until 1/12. The analyses used 12 min as the maximum; longer periods were set to 12 min. In a final step, the whole complementary cumulative density function (CCDF) has been adjusted for a measurement site such that the fine scale interpolated CCDF (in log$p$, $R-p$ the time percentage of a certain rain rate R (mm/h) is exceeded) gives the same total rainfall as observed, i.e., the sum of the differentiated CCDF. See *Mamen and Tjelta* [2013] for a detailed description of the algorithm and some validation using weight pluviometer data to generate/simulate discrete data for testing the algorithm.

For the purpose of radio system diversity improvement, the rain rate distributions are fitted to a lognormal type, and the minimum to the joint lognormal distribution exceedance to derive the rain correlation coefficient used later in the modeling (section 3). An example is shown in Figure 3 for rain rate distribution from Blindern (Station 18701) and Lambertseter (Station 18020), as well as the instantly minimum rain rate, for the full concurrent period of 8 years. In the treatment of the measured data, it is assumed that for the year studied, all heavy rainfall events of about 15–20 mm/h or more have been registered. Therefore, the time series also represents the full year, such that the interpretation is the percent of the average year the rain rate is exceeded. The solid lines show the measured distributions, the broken line shows a lognormal model for part of the distribution from a few mm/h to about 100 mm/h intensities, and the joint density exceedance of rain rates given by the abscissa value. It is seen that the lognormal model compares very well with the measured data for the part of the distributions chosen. The lognormal joint density is [*Papoulis*, 1984]

$$f(x,y) = A\exp\left(-\frac{1}{2(1-\rho^2)}\left[\frac{(x-\mu_1)^2}{\sigma_1^2} - 2\rho\frac{(x-\mu_1)(y-\mu_2)}{\sigma_1\sigma_2} + \frac{(y-\mu_2)^2}{\sigma_2^2}\right]\right) \quad (1)$$

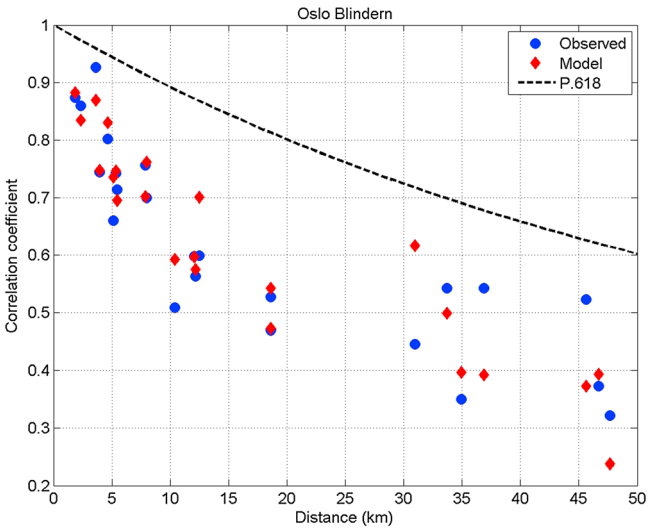

Figure 4. Observed and predicted correlation coefficient of ln(*R*) as function of distance from Oslo Blindern.

where x and y are $\ln(R_1)$ and $\ln(R_2)$ for the two rain rates R_1 and R_2, respectively; μ_1 and μ_2 are the mean values of $\ln(R_1)$ and $\ln(R_2)$; σ_1 and σ_2 are the standard deviation of $\ln(R_1)$ and $\ln(R_2)$; ρ is the correlation coefficient; and

$$A = \frac{1}{2\pi\sigma_1\sigma_2\sqrt{(1-\rho^2)}}$$

The joint lognormal model has just been checked for a narrow region of rain rates around 0.01% of the individual distributions, since this is the main rain rate of consideration for radio system rain attenuation prediction. The derived correlation coefficient used of the joint distribution is shown as well, here ρ is found (rho = 0.799 marked in the figure). This value was used to plot the broken line representation of the joint distribution numerically found using a double integral of equation (1) for both R_1 and R_2 exceeding the abscissa.

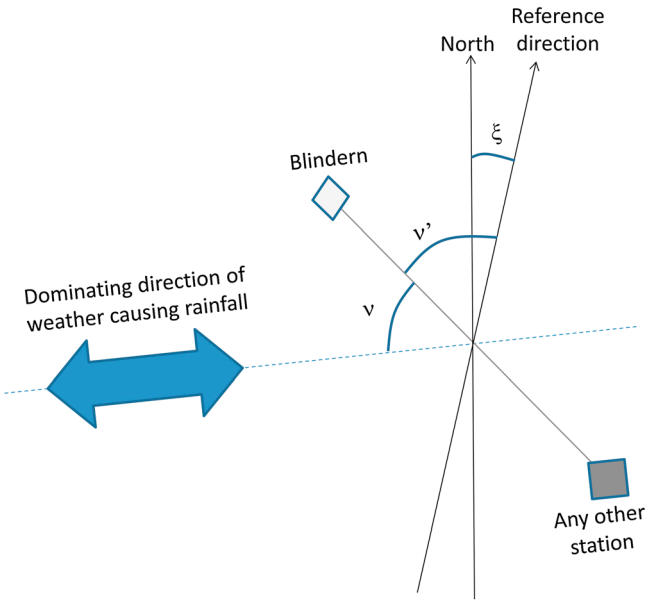

Figure 5. Geometry showing the assuming dominant direction for weather causing medium to high rain rates and the line joining two tipping bucket rain gauges.

The correlation coefficient ρ has been derived from fitting the measured to the joint distribution of the two lognormal distributions. Here each set of mean and standard deviation has been estimated from the measured individual distributions, and the correlation coefficient of equation (1) numerically found by minimizing the deviation from the calculated joint lognormal distribution and the measured, i.e., minimizing $\Sigma\log(p_{calc}/p_{meas})$, where p_{calc} is the percentage calculated and p_{meas} is the percentage measured at a number of selected values.

The alternative of calculating the correlation coefficient from the full concurrent time series data results in too low values, such that the joint exceedance around the more significant rainfall rates exceeded for

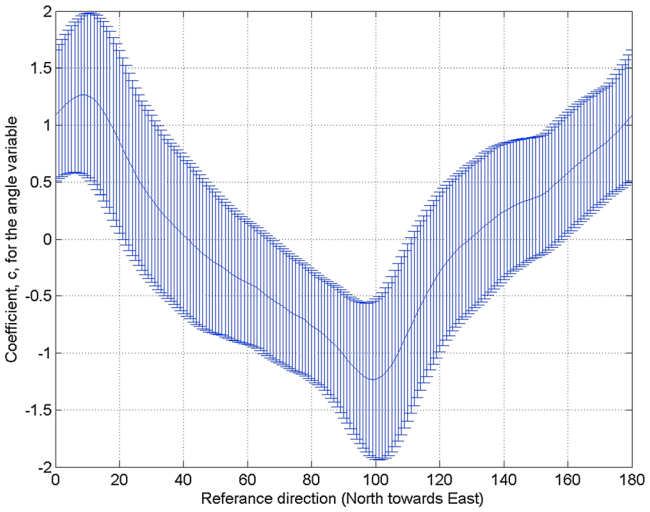

Figure 6. Coefficient for the angle variable, c, with confidence intervals plotted for varying reference line directions given by ξ.

0.01% of the time for the individual links becomes too low compared with measurements. It may be that the discrete time series data are not suitable to retrieve the correlation coefficients directly.

The analysis of simultaneous rain rate data for all pairs of stations with one at Blindern and each of the others in turn gives information on spatial correlation of rainfall intensity. Figure 4, blue dots show the derived measured correlation coefficients ρ as the function of distance from Blindern. It is noted that the correlation coefficient quite quickly reduces, in fact considerably more than suggested in P.618 shown as well. Figure 4 also demonstrates that there is variability of ρ at the same distance. The model, shown as red diamonds, is developed to predict the variability, as well as the primary function of separation distance. See the next section for the development of this model.

3. Prediction Model for Rain Rate Correlation Coefficient

The correlation coefficient must be close to 1 when the separation of stations is small. At very large distances, it will be small or perhaps even negative. For the fairly small area under study, it is assumed to follow the ideas of joint bivariate lognormal distributions and vary between 1 and 0. Apart from separation distance, it is reasonable that angle with a dominating weather direction for the heavy rainfall will play a role, if such a dominating direction is present in the region. Figure 5 illustrates the geometry assuming a dominating weather direction exists and with two rain gauge locations indicated to derive the distance and angle used. The figure depicts two rain gauge stations. One is Blindern and then one other. There are 23 such pairs. The direction of a potential dominant weather direction is given; hence, the angle's baseline between the rain gauges and the weather direction is defined (v). In the search for a possible dominating weather direction, the help line called reference direction and two new angles v' and ξ are used, also shown in the figure.

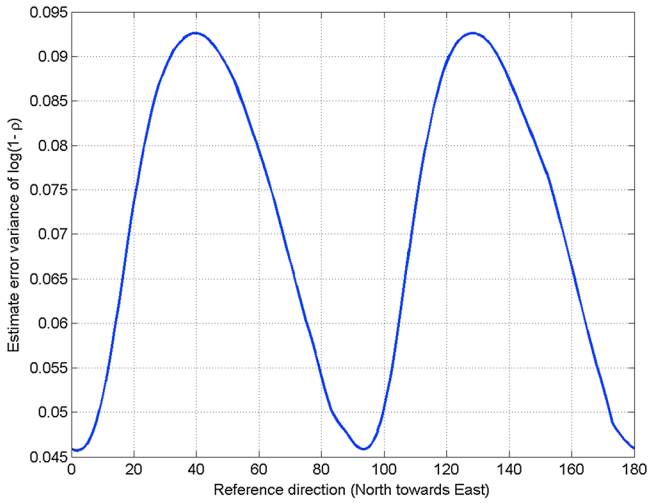

Figure 7. Estimate error variance of the prediction model, i.e., the predicted exponent of equation (2), as a function of stations connected line alignment.

Then the following model for ρ is suggested and investigated:

$$\rho = 1 - a' d^b \left(1 + \frac{v}{90}\right)^c \qquad (2)$$

where d (km) is the separation distance, v (deg) is the angle with the dominating weather direction and the line connecting the rain gauges, and a', b, and c are the constants. The variable v is the absolute value of the smallest angle such that it will be between 0 and 90°. It simply determines to what degree the weather direction is parallel or perpendicular to the line between the rain gauges.

Table 2. Regression Model Coefficients, i.e., *a*, *b*, and *c* in Equation (3)

	Coefficients	
Variables	Two Variables	One Variable
Constant	−2.869	−2.288
ln(*d*)	0.504	0.488
ln(1 + *v*/90)	1.247	
Estimated error variance	0.046	0.088

The main parameter in determining ρ is likely the separation distance, the only parameter used, e.g., in P.618. In equation (2), the effect of v will be to increase ρ from its minimum when the line between the sites in question is aligning with the dominant direction of weather for negative *c* or reduce ρ if *c* is positive.

By taking the logarithm of equation (2), it is seen that $\ln(1-\rho)$ can be found by using multiple linear regression analyses to calculate the constant *a* and variable coefficients *b* and *c*:

$$\ln(1-\rho) = a + b\ln d + c\ln\left(1+\frac{v}{90}\right) \tag{3}$$

where $a = \ln(a')$.

The first analysis presented [*Tjelta et al.*, 2013] used the inverse of diversity improvement for the area rain intensity reduction as observed from Figure 3 for single station rain rate exceeded at 0.01%, but here in this article, the correlation coefficient is analyzed since this is the input variable used for site diversity prediction [*ITU-R*, 2013a].

Since it is not known whether a dominating direction exists, and what the angle v should be in such a case, the procedure followed is to choose angles ξ of a reference line deviation from north and then calculate an angle v' with respect to the reference line for all station pairs. By stepping ξ from 0 to 360°, a new regression model with coefficients *a*, *b*, and *c* are found for each reference direction. Then, if there is a dominating weather direction, it will be seen from the regression models, i.e., the prediction model that has the lowest estimated error variance and still a confident variable v.

The ρ model function of distance is slightly more complex in P.618 with two terms, but each term only based on separation distance. With the simple power law form suggested in this article, regression models can be derived both using only separation distance *d* as one variable and as a two-variable model including angle v in addition. For the short distances up to 50 km, the P.618 is dominated by the first term.

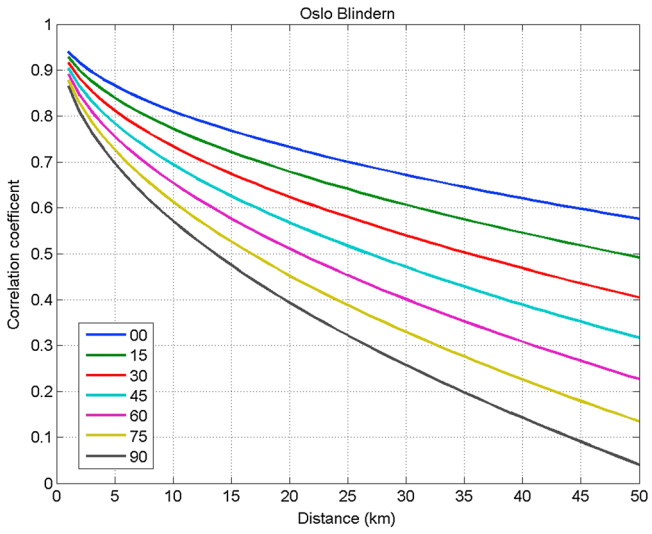

Figure 8. Correlation coefficient ρ_{rain} as a function of distance and angle to a reference direction of 2° found by regression analyses of rain gauge data in the Oslo region.

By selecting reference lines given by ξ from 0 to 180°, the regression coefficients are found. The coefficient and its 95% confidence limits for the second variable $\ln(1 - v'/90)$ are plotted in Figure 6. Due to symmetry, it is not necessary to calculate the coefficients for the whole circle up to 360°; in fact, it would be enough to stop at 90° or even 45° if more data had been available. But it is instructive to see the coefficients until 180°. The confidence limits in Figure 6 show two regions with "confident models" for the two-variable fit: one between about −25° (155° in the figure) and 20° and another between about 65° and 110°. With a confident direction variable, it

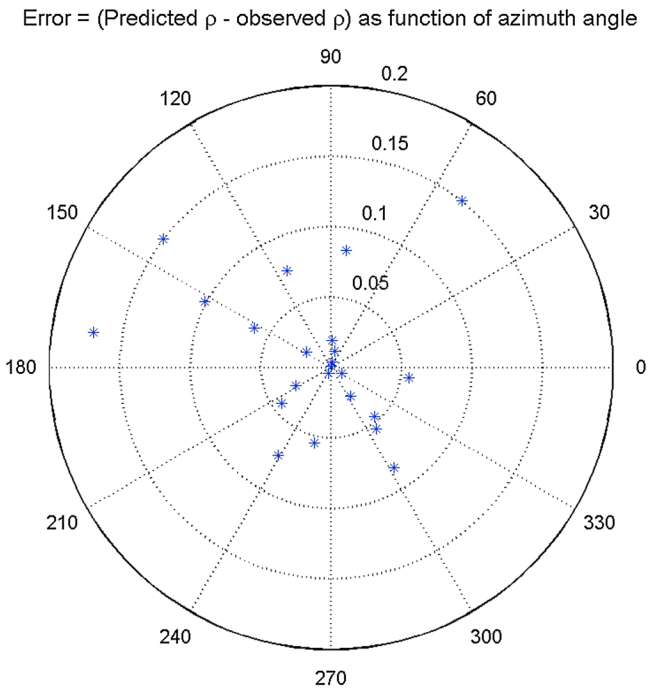

Figure 9. Prediction error of the two-variable regression model as a function of azimuth angle.

means that there is a plausible dominant weather direction given by the reference line within either of these two regions.

The model suggests that there should be a 90° shift between each useful reference line for the main weather direction, as also seen in the plot of estimated error variance in Figure 7. The minimum estimated error variance identifies the best regression models at 2° and similarly 92°. Although not easily seen from Figure 6, at these angles, the coefficient confidence ranges are also smallest.

The results of one-variable regression model and two-variable regression model for minimum standard estimated error variance are given in Table 2.

The interpretation of the two-variable model is that a 2° angle for the reference line results in the highest correlation for v equals 0° and that the correlation is reduced until its minimum for v equals 90°. Therefore, the dominating weather causing heavy rainfall follows a west-east line given by 92° or 272° azimuth angle measured from north. The correlation coefficient is plotted for various angles referenced to the 2° line in Figure 8, where it is seen that the lowest correlation is for the 90° difference.

The two-variable model performs fairly well concerning prediction error as function of angle with the reference direction of 2° as seen in Figure 9. The correlation as function of separation distance and angle is given by using the coefficients in Table 2

$$\rho = 1 - 0.056d^{0.504}\left(1 + \frac{v}{90}\right)^{1.247} \tag{4}$$

The prediction errors distribute fairly evenly with azimuth angle; i.e., the angle the line between rain gauges sites make with north (positive north toward east).

A similar two-variable model with reference line if $\xi = 92°$ gives the same low estimated error variance as the model given in Table 2, but the coefficient c is negative. For practical purposes, to use the new site diversity model, the dominant weather direction must be identified. In the next section, one possible method is given.

4. Local Meteorological and Climate Variability

This section presents the climate of the region in order to better understand the findings in the previous section. It also suggests analysis of upper air radiosonde data to find a possible dominant weather direction.

In summer, the Oslo area is among the warmest in Norway, with mean temperatures for the warmest month in the range of 14–17°C, depending more on altitude than distance from the Oslofjord. While summer precipitation is high, autumn is usually the wettest season. Typical for summer is heavy showers, with large variations in intensity over short distances.

From the meteorological and climatological sides, the wind direction at 850 hPa or 700 hPa air pressure is indicating the direction of the weather at the ground. These altitudes correspond to about 1500 m or 3000 m heights above the sea level, respectively. For example Shearman states [*Shearman*, 1977] that it is a commonly accepted empirical rule in meteorology that storm rainfall moves approximately with the

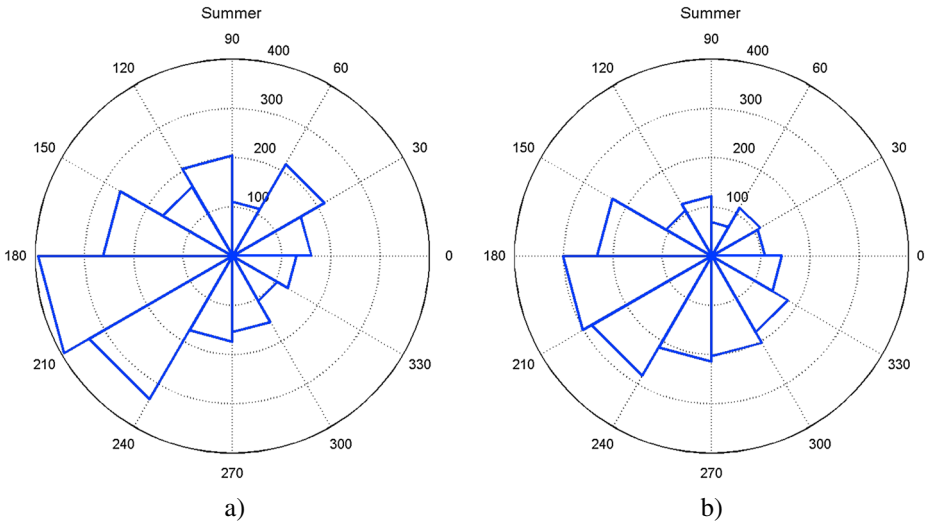

Figure 10. Wind rose from north at 0° toward east observed for summer months June, July, and August using radiosonde data at Gardermoen from the period of 1967 to 2001, observed at (a) 850 hPa and at (b) 700 hPa.

700 hPa wind. However, not all cellular rainstorms did follow the 700 hPa wind field. In another paper, *Pestaina-Haynes and Austin* [1976] found that rain storm directions in the tropics, Barbados, and Montreal did follow the wind direction at 1000 hPa, 850 hPa, and 700 hPa, respectively. *Warren et al.* [2013] used the mean of wind speed and directions at 700 hPa and 850 hPa as an indicator for quasi-stationary convective precipitation movement direction at ground. Also, the company *Weatherzone* [2013] explains that the wind at 850 hPa shows the direction of lower level systems and the wind at 700 hPa is a good estimator for thunderstorm movement direction. However, the wind at the ground will vary more and will not necessarily align with the direction in the 700 hPa or 850 hPa level.

There are radiosonde data available from Gardermoen until the end of 2001, which is within the 50 km radius of Blindern, and has one of the rain gauges as well. Using data from the period of 1967 to 2001, Figure 10 shows a wind rose for Gardermoen for the summer months as observed by radiosondes at 850 hPa height, showing that the most frequent wind direction is south or southwest. For the following results, the wind speed and direction at 850 hPa and 700 hPa were used if the relative humidity was larger than 70%. Furthermore, data with wind speed equal to 0 m/s were not included either.

It is expected that intense rainfall will happen if thunderstorms are likely. The thunderstorm *k* index is an indicator that higher values increase the possibility of thunderstorms and heavy rainfall. It is defined as [*George*, 1960]

$$k = t_{850} - t_{500} + t_{d850} - (t_{700} - t_{d700}) \tag{5}$$

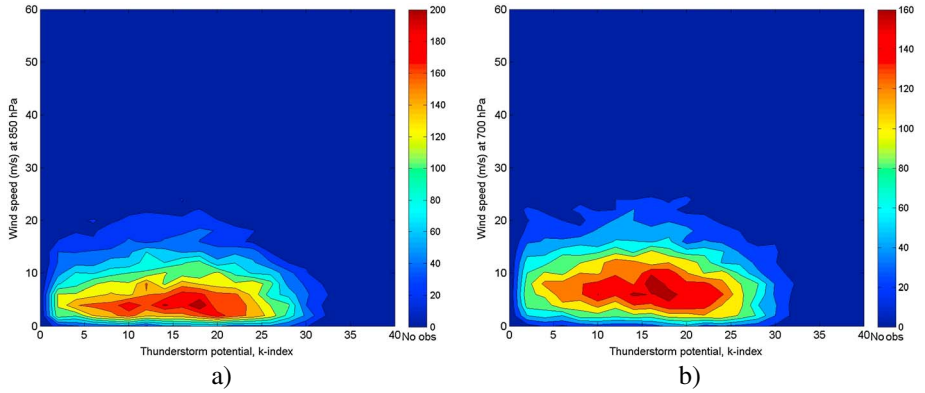

Figure 11. Scatterplot of wind speed at pressure heights (a) 850 hPa and (b) 700 hPa and thunderstorm index *k*.

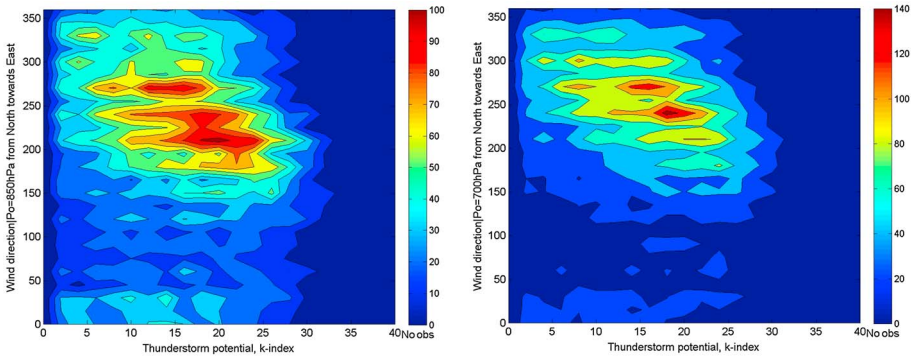

Figure 12. Joint histogram of wind direction from north at 0° toward east and the thunderstorm index *k* for pressure heights (a) 850 hPa and (b) 700 hPa.

where *t* is the temperature at the pressure height (hPa) given by the subscript and t_d is the dew point temperature also at the pressure height (hPa) given by the subscript. All these temperatures are available as standard reported values from radiosonde ascents. Also, other "heavy rain indicators" may be considered, such as high temperature difference between the ground and the 850 hPa level.

Figures 11 and 12 show the wind speed and the wind direction at the 850 hPa and 700 hPa altitudes as functions of *k*. In selecting data for comparison with the thunderstorm *k* index, only values larger than 0 were included. It is noted that the wind speed seems to reach maximum *k* index values around 15 to 20. For the lowest *k* values, Figure 12 indicates more wind directions from 250° to 300° than other azimuth angles, but the maximum number of observations seems to peak around 20 and a direction in the range of 200 to 250.

Figure 10 indicates that southerly winds are most frequent at both 850 hPa and 700 hPa and that the amount of westerly winds increases from 850 hPa to 700 hPa. In section 3, the lowest correlation for simultaneous precipitation was found by weather systems following a west-east line given by an azimuth angle of 92° or 272°. For this direction, Figure 12b shows *k* indexes at 700 hPa between 15 and 20 and wind directions between 240° and 270°. Climatologically, this means weather systems with moderate or heavy precipitation moving from west to east.

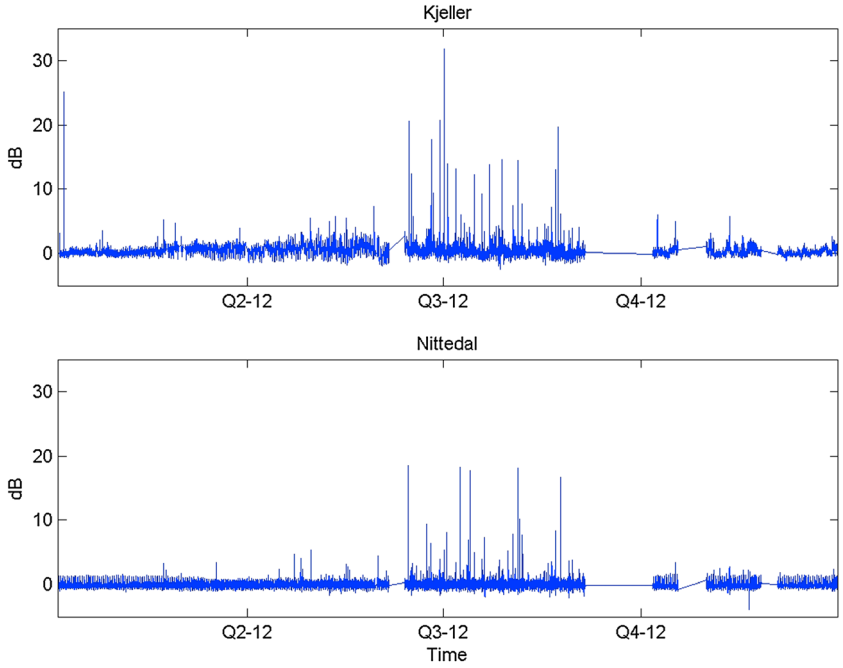

Figure 13. Concurrent 20 GHz attenuation time series data of 2012 measured at Nittedal and Kjeller.

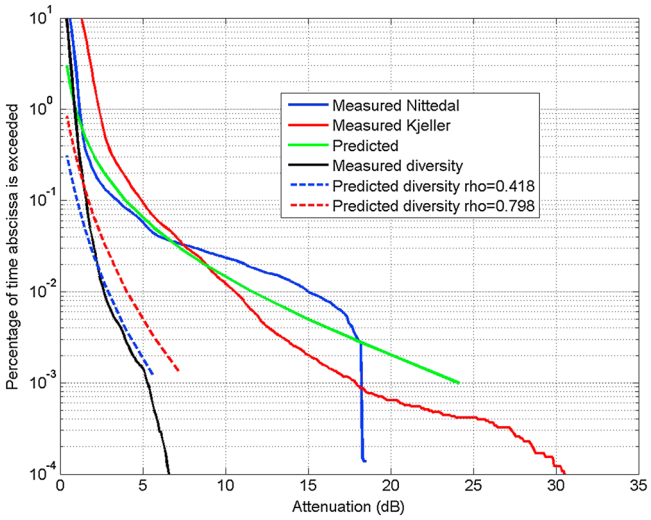

Figure 14. Measured and predicted excess attenuation distributions for Nittedal, Kjeller, and the minimum (diversity). The diversity curve with the highest predicted percentage is achieved using ρ_{rain} from P.618 and the lowest using the model in this article.

5. Measured Site Diversity Improvement

This section provides an initial analysis of site diversity data from the region. It uses P.618 site diversity prediction with the revised rain correlation coefficient measurement data: from one station at Nittedal and the other at Kjeller, see Figure 1.

Telenor Satellite Broadcasting launched the Thor 5 satellite in 2008 into location 1°W to provide broadcast and data services in the Nordic and central Europe. Nittedal Teleport, located north of Oslo, Norway, is the main uplink station for Thor 5.

All broadcast transponders on Thor 5 are illuminated with a broadband single carrier (DVB-S/DVB-S2). A power detector circuitry in the satellite high-power amplifier is recording the power level at the input of the satellite repeater. The measured level is transmitted to the ground station via telemetry link and archived in the on-ground control center. In addition to propagation effects, the power estimate is influenced by diurnal gain variations. These daily variations are postprocessed and filtered out in the data set.

The center frequency of the investigated uplink signal is 18.0 GHz, and the total bandwidth is 33 MHz.

Measured telemetry data at Nittedal from the Thor 5 satellite at 1°W and the 19.3 GHz beacon data at FFI, Kjeller, from the Astra 4A satellite at 4.8°E have been used to check for diversity improvement using these two sites that are separated about 23 km. Both sites are in the Oslo region and within the area covered by network of tipping bucket rain gauge data available from the Norwegian Meteorological Institute. See *Bråten and Tjelta* [2013] for detailed information on the measured Kjeller data.

Figure 13 shows the concurrent time series of 20 GHz attenuation at Nittedal and Kjeller measured in 2012. The dynamic ranges are about 18 dB for Nittedal and more than 32 dB for Kjeller. There are gaps in the data, here visible as straight lines close to 0 dB. The minimum sampling rate was 4 s given by the Thor 5 data. Actually, only changes have been stored, such that the time between measurements varied. For the diversity study in this article, the signal strength Thor 5 values in between time periods longer than 4 s were interpolated, except for the data gaps either resulting from the Thor 5 data or the Astra 4A data.

The Nittedal data have been filtered to remove a significant daily variation caused by nonpropagation effects, and the reference for Kjeller data is the monthly median. The attenuation distributions given in Figure 14 have been derived from the concurrent time series data for both sites and the minimum attenuation at any instant to get the diversity improvement or gain. The limited dynamic range of Nittedal is quite visible, but for the purpose of diversity analysis, it has no negative effect as seen from the diversity signal distribution.

Figure 14 also depicts the predicted rain attenuation distribution at Nittedal and diversity distributions. ITU-R P.618 [*ITU-R*, 2013a] provides a prediction method for site diversity distributions. Using this method with rain rate of 28 mm/h exceeded at 0.01% of the time but with rain correlation coefficient $\rho_{rain} = 0.418$ derived from tipping bucket measurements with separation distance of 23.0 km and separation angle of 35.9°. The correlation coefficient is significantly lower than 0.798, the value to use if P.618 is strictly followed.

The measured and predicted single link distributions compare to some extent, but the limitation of fade margin is visible for the Nittedal link and probably also effects from the different methods for setting the 0 dB reference. There are, as well, some differences between the sites, although noted, it is not the subject of this article to go further into details for these variations. The measured diversity is limited to maximum 7 dB, probably caused by both the limited margin for the Nittedal link and the short

measurement period. However, up to 5 dB of the distribution is reasonably described by the predicted diversity distribution where the correlation derived from the local rain rate data clearly provides a much closer fit.

6. Discussion and Conclusion

Site diversity is used for satellite systems to ensure satisfactory service delivery. For example, uplink broadcast services must be very well protected against failures. Then it is important to ensure satisfactory improvement for failures caused by propagation effects such as rain attenuation. In the same manner, terrestrial high-frequency mesh networks may improve the network performance by deploying route diversity.

Rain intensity correlation is a key in achieving improved availability using multiple links in diversity setup as protection against rain attenuation. Therefore, the rain correlation coefficient is also used directly as part of the method recommended for satellite site diversity improvement prediction in P.618. The results in this article show that the correlation is different depending on both separation distance and the angle the site connection line forms with a reference line. Obviously, a prediction method is only needed when there is no satisfactory or any observed local information available. The most important variable distance separation d in the model of correlation is readily available, of course, but the second angle v is not. The two-variable regression model suggests that the correlation is highest if the stations are lined up with the 2°–182° direction referenced to north toward east and smallest at a line perpendicular to this at 92°–272°. The study of radiosonde data suggests that the dominating wind direction for thunderstorm index around 20 may identify the proper reference line used for smallest correlation coefficient. This means that it would be better to align base station sites along the direction of the weather system than perpendicular to it. This article points at the prevailing wind at 850 hPa or 700 hPa heights conditioned at thunderstorm index around 15–20. This was found to be around 240°–270°, and one value shows that 255° could be used as dominating direction instead of 272°.

The site diversity prediction method investigated in this paper was introduced in recommended method P.618 in 2007 in version 9, based on a proposal in an input document from 2003 [*ITU-R*, 2003]. The document refers to proposals made by *Paraboni and Barbaliscia* [2002] to use lognormal distributions for rain intensity and attenuation to derive the site diversity improvement. Since lognormal distribution was suggested by *Lin* [1973], it has been utilized in many rain attenuation data analyses. Paraboni and Barbaliscia point out that the lognormal distribution representations are well established for the shallower attenuation range and the distribution fits well with the rain intensity observations discussed in this paper. Therefore, the correlation coefficients have been derived from the important part of the measured diversity distributions rather than using the time series data that resulted in too low estimates of correlation coefficients.

Several contributions have been published supporting diversity improvement for separation distances within a 50 km range. *Rogers and Allnut* [1984] present a study of multiple experiments pointing out the importance of convective rainfall. *Roy et al*. [2011] actually indicate that very short separation distances of a few hundred meters still result in some improvement, as did *Acosta et al*. [2013]. However, it may well be that a lognormal distribution is not the best choice and that perhaps other climate parameters should be included as well where neither follows a normal or lognormal distribution. *Kourogiargas et al*. [2012] suggest bivariate inverse Gaussian distributions. Future work should consider multivariate distributions where these are not normal (or lognormal). One such approach seems to be what is called copula distributions, see, e.g., *Schötzel and Friedrichs* [2008] for an introduction. *Craig* [2007] deployed copula distributions for an analysis of clear-air fading and enhancement on radio links and a recent paper by *Kourogiorgas et al*. [2014] actually tried some functions with interesting results.

It remains a challenge to precisely find a dominating weather direction for the purpose of improved rain correlation modeling. Early work utilizing radar data indicates little dependency on site alignment [*Goldhirsh*, 1978] or some with orientation of elongated rain cells [*Hodge*, 1976]. A more recent study by *Luini et al*. [2011], also based on radar data, points at the average wind direction at 700 hPa as a good indicator. In looking for refined rain attenuation modeling, *Silva Mello et al*. [2013] suggested to use wind derived from numerical weather data such that a similar source for wind direction may also well be found useful for the rain correlation case.

The ITU-R handbook on Earth to space propagation discusses to use site diversity protection and comment on prevailing direction of weather systems [*ITU-R*, 1996]. However, the view expressed for short separation distances to select the baseline connecting the two sites in question to preferably align perpendicular to the weather systems seems to be opposite to what has been found in this article.

In conclusion, this article has shown that shorter than 50 km separation distances between sites may result in significant reduction of rain rate correlation using a large number of long-term tipping bucket rain gauges. It has developed a relation between separation distance and prevailing direction for rain weather and identified a possible independent source to identify the prevailing direction. The 1 year satellite-measured data at 20 GHz indicate that the findings are on the right track, indicating that the current prediction method in P.618 is too pessimistic and its accuracy can be increased by including prevailing weather direction.

Acknowledgments

The rain rate data and radiosonde data analyzed for the work in this paper are publicly available by the Norwegian Meteorological Institute. The easiest access is via the second author from the institute, but part of such data is also made available for free access through the Web site eklima (eklima.met.no). The set of satellite data measured by FFI at Kjeller is part of an ongoing measurement research project, and the time series data are not publicly available. The time series data by the satellite Thor 5 obtained by Telenor Satellite Broadcasting are to some degree commercial sensitive information and cannot be made available publicly.

References

Acosta, R. J., E. Matricciani, C. Riva (2013), Slant path attenuation and microscale site diversity gain measured and predicted in Guam with the synthetic storm technique at 20.7 GHz, in Conference proc. of EuCAP, 8-12 April.

Bråten L. E., and T. Tjelta (2013), Planned and early results of low elevation angle measurements at Ka-band from two projects in Norway, *CNES-ONERA International Workshop*, Toulouse, France, 21–23 Jan.

Craig K. H. (2007), A methodology for modelling the correlation of fading and enhancement on radio links, in *Conference proc. of EuCAP*, 11–16 Nov.

George, J. J. (1960), *Weather Forecasting for Aeronautics*, pp. 673, Academic Press, New York.

Goldhirsh, J. (1978), Path attenuation statistocs influenced by orientation of rain cells, IEEE TAP, AP-24, pp. 792–799.

Hodge, D. B. (1976), Path diversity of earth-space communication links, pp. 481–487, 13 May-June.

ITU-R (1996), Radiowave Propagation Information for Predictions for Earth-to-Space Path Communications, in *International Telecommunication Union*, *Handbook*, edited by C. Wilson and D. Rogers, ITU, Geneva, Switzerland.

ITU-R (2003), Working document toward a revision to the site diversity prediction method in Recommendation ITU-R P.618-8, International Telecommunication Union, ITU-R Document 3M/35 (2002–2005), Geneva, Switzerland, 13 November.

ITU-R (2012), Propagation data and prediction methods required for the design of terrestrial broadband radio access systems operating in a frequency range from 3 to 60 GHz, International Telecommunication Union, Recommendation P.1410-5, Geneva, Switzerland.

ITU-R (2013a), Propagation data and prediction methods required for the design of Earth-space telecommunication systems, International Telecommunication Union, Recommendation P.618-11, Geneva, Switzerland.

ITU-R (2013b), Propagation data and prediction methods required for the design of terrestrial line-of-sight systems, International Telecommunication Union, Recommendation P.530-15, Geneva, Switzerland.

Kourogiorgas, C. I., A. D. Panagopoulos, and J. D. Kanellopoulos (2012), On the Earth-Space site diversity modeling: A novel physical–mathematical outage prediction model, *IEEE Trans. Antennas Propag.*, *60*, 4391–4397.

Kourogiorgas C. I., S. N. Livieratos, A. D. Panagopoulos, and G. E. Chatzarakis (2014), Modeling of joint rainfall rate and rain attenuation statistics using Archimedean copula functions, in Conference proc. of EuCAP, 7–11 April.

Lin, S. H. (1973), Statistical behavior of rain attenuation, *Bell Syst. Tech. J.*, *52*(4), 557–581.

Luini, L., N. Jeannin, C. Capsoni, A. Paraboni, C. Riva, L. Castanet, and J. Lemorton (2011), Weather radar data for site diveristy predictions and evaluation of the impact of rain field advection, *Int. J. Satell. Commun. Network.*, *29*, 79–96.

Mamen J., and T. Tjelta (2013), New Norwegian hydrometeor precipitation rate maps derived from long term measurements, in *Proceedings of EuCAP 2013*, 8–12 April, Gothenburg, Sweden.

Papoulis, A. (1984), *Probability, Random Variables, and Stochastic Processes*, 2nd ed., McGraw Hill, Singapore.

Paraboni A., and F. Barbaliscia (2002), Multiple site attenuation prediction models based on on the rainfall structures (meso- or synoptic-scales) for advanced TLC or broadcasting systems, *in Proc. Of XXVIIth General Assembly of the International Union of Radio Science*, Maastricht, Netherlands.

Pestaina-Haynes, M., and G. L. Austin (1976), Comparison between maritime tropical (GATE and Barbados) and continental mid-latitude (Montreal) precipitation lines, *J. Appl. Meteorol.*, *15*, 1077–1082.

Rogers, D. V., and J. E. Allnut (1984), Evaluation of a site diversity model for satellite communications systems, *IEE Proc.*, *131*(5), pp. 501–506.

Roy, B., A. K. Shukla, and M. R. Sivaraman (2011), Micro scale site diversity over a tropical site in India and evaluation of diversity gain with synthetic storm technique, *Indian J. Radio Space Phys.*, *40*, 211–217.

Schölzel, C., and P. Friederichs (2008), Multivariate non-normally distributed random variables in climate research – Introduction to the copula approach, *Nonlinear Process Geophys*, *15*, 761–772.

Shearman, R. J. (1977), The speed and direction of movement of storm rainfall patterns with reference to urban storm sewer design, *Hydrol. Sci.*, *XXII*(3), 421–431.

Silva Mello L. d., F. Andrade, M. P. C. Almeida, and M. S. Pontes (2013), New approaches for the prediction of rain attenuation in terrestrial line-of-sight links, *Abstract 13th URSI Commission F Triennial Open Symposium on Radiowave Propagation and Remote Sens.*, Ottawa, Canada, 30 April – 3 May.

Tjelta T. and J. Mamen (2014) ,Climate Trends and Variability of Rain Rate Derived from Long Term Measurements in Norway, *Radio Sci.*, *49*, 788–797, doi:10.1002/2014RS005477.

Tjelta T., J. Mamen, L. E. Bråten, and P. A. Grotthing (2013), Spatial rain rate variation derived from long term measurements in the Oslo region of Norway for radio system diversity improvement, Abstract *13th URSI Commission F Triennial Open Symposium on Radiowave Propagation and Remote Sens.*, Ottawa, Canada, 30 April – 3 May.

Warren R. A. , R. S. Plant, D. J. Kirshbaum, and H. W. Lean (2013), A Climatology of Heavy Rain-Producing Convective Systems in the UK, poster in *Proc. of AMS 15th Conference on Mesoscale Processes*, Portland, OR, 6–9 Aug.

Weatherzone (2013), How to read the charts. [Available at http://www.weatherzone.com.au/help/article.jsp?id=49, 14 September 2013.]